Optimization of Direct Metal Laser Sintering Parameters to Produce Crack Free Alloy 230

PURDUE MATERIALS ENGINEERING

Ziyu Cai, Jack Lopez, Cory Richards, Philip Spagnolo, Katie Thomas
Faculty Advisor: Dr. Xinghang Zhang
Industrial Sponsor: Bill Jarosinski

Alloy 230, a NiCr Alloy often experiences detrimental cracking when manufactured using Direct Metal Laser Sintering (DMLS). Therefore, the goal of this project was to optimize the DMLS parameters to reduce cracking. Three sample sets, named DOE 1, DOE 2, and DOE 3, were built. DOE 1 was built according to the parameters used prior to this project and exhibited severe cracking in all samples. DOE 2 was designed with lower power input and layer thickness and exhibited very little cracking. DOE 3 attempted to decrease production time by increasing layer thickness, but resulted in samples being either cracked or porous.

This work is sponsored by Praxair Surface Technologies, Indianapolis, IN

PRAXAIR SURFACE TECHNOLOGIES

Project Background

The DMLS process has four main parameters: laser power, scanning speed, hatch spacing, and layer thickness. Figure 1 illustrates how each of these parameters contributes to the process. These variables can be summarized by the energy density value as seen in Equation 1.

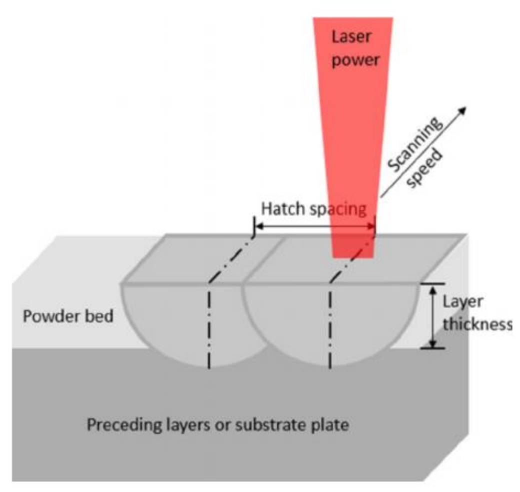

Figure 1: Schematic representation of DMLS parameters.[1]

$$\psi = \frac{P}{v*d*h}$$

Equation 1: Energy Density (Ψ) equation. *P* is the laser power, *v* is the scan speed, *h* is the layer thickness, and *d* is the hatch spacing.

Alloy 230 is used in multiple aerospace applications, such as engine components. Alloy 230 is extremely resistant to high-temperature creep and corrosion, making it ideal for these applications. Tungsten and molybdenum additions create high-temperature creep and corrosion resistance.

Table 1: Weight Fraction of Elements present in Alloy 230

Element	Ni	Cr	W	Mo	Fe	Co	other
wt%	<57(bal)	22	14	2	< 3	< 5	< 3

Optical/Crack Density

DOE 1

- Optical imaging of original Praxair samples showed cracks uniformly distributed across the surface.
- Crack density calculations were performed for all samples and showed that as the energy density increased, the number of cracks decreased.

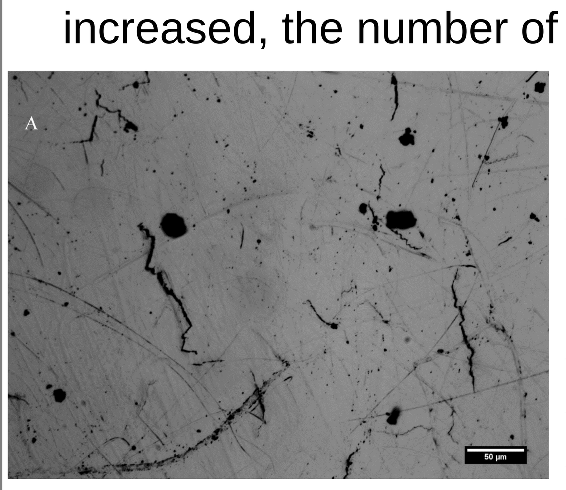

Figure 2: Optical image of sample from DOE 1 with an energy density of 139 J/mm³.

Table 2: Average crack density values for the different energy densities in DOE 1.

Energy Density (J/mm³)	Avg. Crack Density (% of Total Area)
139.2	2.07
113.4	3.37
92.8	2.25
75.9	2.20
61.8	2.11

DOE 2

- Samples produced under the Bauer et al. conditions [2] used 200W laser power and 30μm layer thickness with similar energy densities to those in DOE 1 but showed little to no cracks across the surface.

DOE 3

- Samples had an increased layer thickness from samples in DOE 2 and displayed inhomogeneous cracking across the surface.
- Samples at lower scan speeds had a high density of voids. As the scan speed increased, the crack density of samples increased.

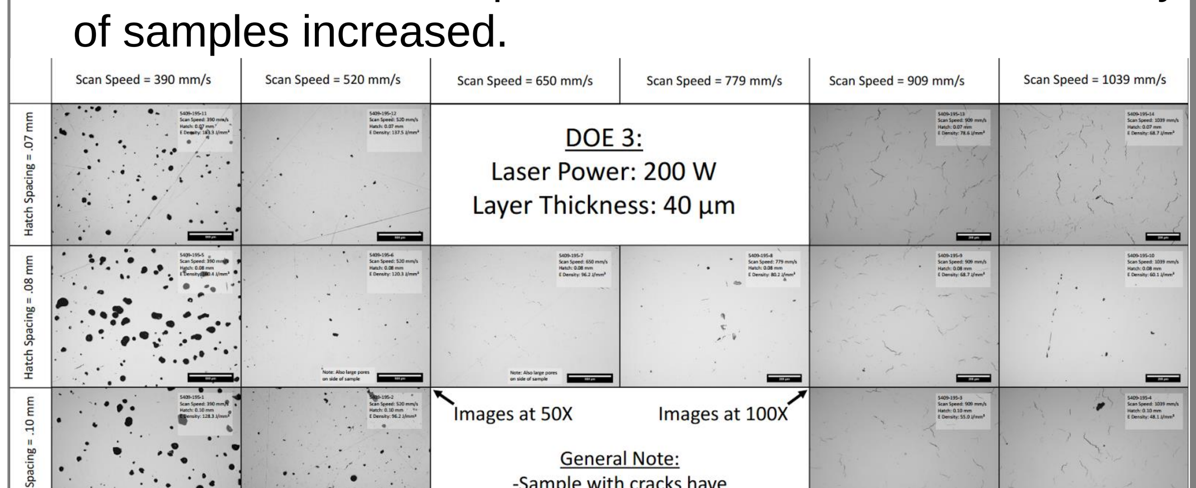

Figure 3: Micrograph overview corresponding to parameter matrix of samples in DOE 3.

Scanning Electron Microscopy / Energy Dispersive Spectroscopy

Scanning Electron Microscopy (SEM) was used to observe crack morphology at higher magnifications. Crack morphology was consistent across all three DOEs in samples that showed cracks. Backscatter electron (BSE) imaging showed no phase contrast.

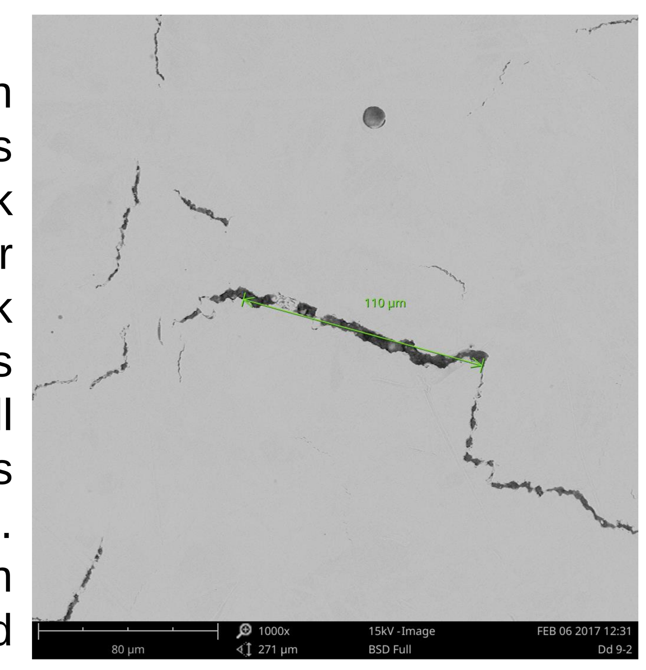

Figure 4: SEM image of a sample from DOE 1, displaying the morphology of a typical crack observed in DMLS-fabricated Alloy 230.

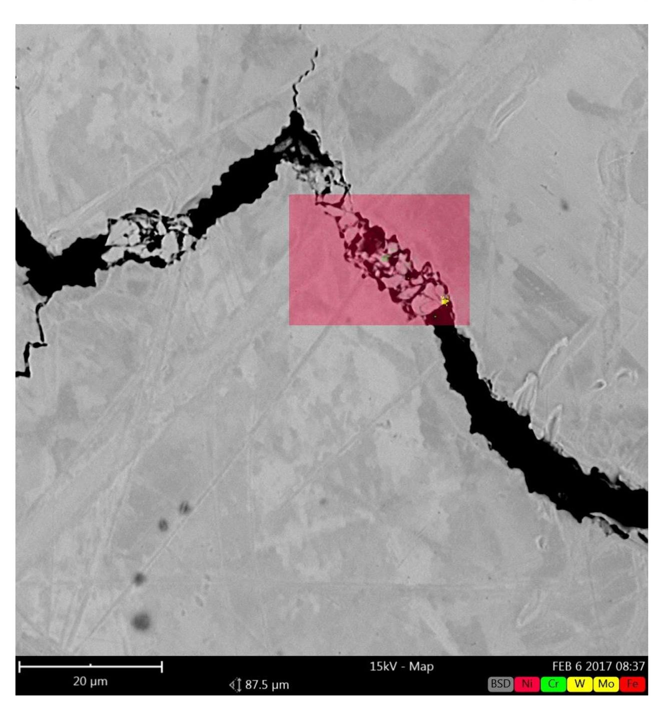

Figure 5: SEM image of a sample from DOE 1, overlaid with EDS mapping of Nickel, Chromium, Tungsten, Molybdenum, and Iron.

Energy dispersive spectroscopy (EDS) capabilities of the Phenom desktop SEM were used to confirm or deny the presence of stress-concentrating carbides or elemental segregation near cracks. Across samples from each DOE, no particles with measurably different compositions were found and no elemental segregation was seen near cracks.

X-ray Diffraction

DOE 1 had a range of spectra that all showed the [200] peak overwhelming the [111]. Preferential grain orientation in the [200] may correspond to the vast amount of cracks present. Considered to be 'worst-case scenario.'

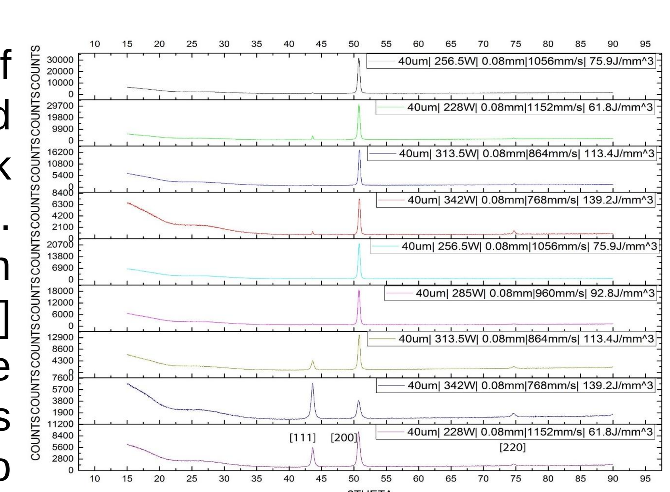

Figure 6: XRD spectra of DOE 1 with legend showing sample's conditions.

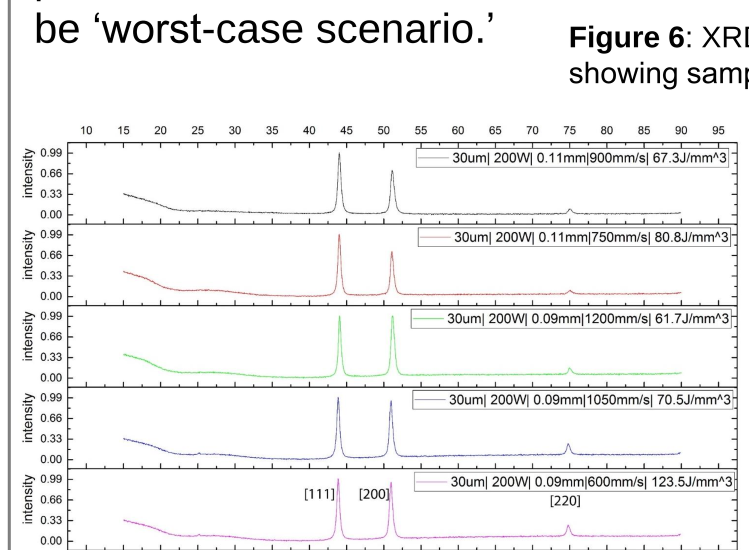

Figure 7: XRD spectra of DOE 2 with legend showing sample's conditions.

DOE 2 showed spectra with the [111] intensity slightly larger than the [200]. Considering this DOE showed little to no cracks, these spectra would be considered as the ideal.

DOE 3 resulted in an average between DOEs 1 and 2, showing both good and bad results. Best results were around hatch spacing of 80μm with progressively worse results as the hatch spacing strayed away from 80μm.

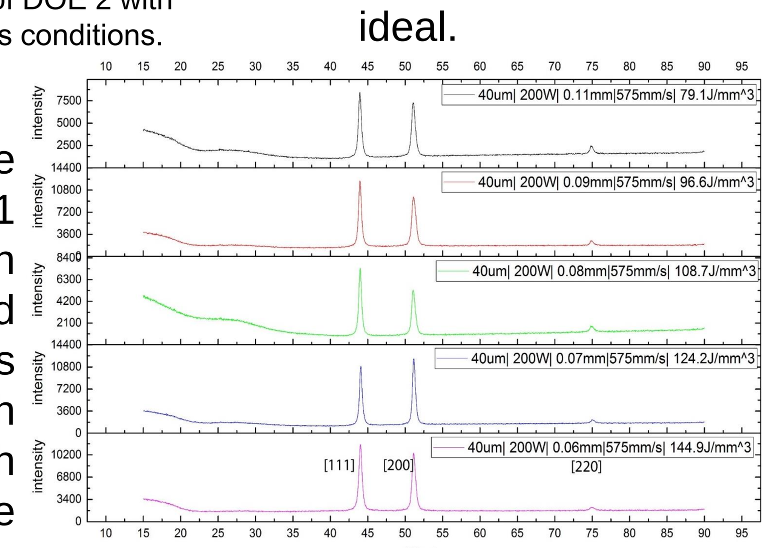

Figure 8: XRD spectra of DOE 3 with legend showing sample's conditions.

Conclusions

DOE 1 samples exhibited extreme cracking which could lead to failure, especially in fatigue applications. DOE 2 samples, produced with the Bauer et al. paper conditions, had far fewer cracks than DOE 1 samples, if any. Samples run using 30μm layers (only seen in DOE 2) were the only samples produced without cracks. While it is believed that lower laser power is beneficial, 30μm layer thickness is the only condition solely associated with the successful samples.

DOE 3 kept similar laser power as DOE 2 (200W), but increased the layer thickness back to 40μm in order to decrease production time. Despite the change to lower laser power, cracks were still observed in the majority of samples. Additionally, samples with higher energy densities showed large voids while samples with lower energy densities demonstrated heavy cracking similar to that seen in DOE 1. Energy densities from 70 J/mm³ to 80 J/mm³ had the fewest cracks and the smallest voids.

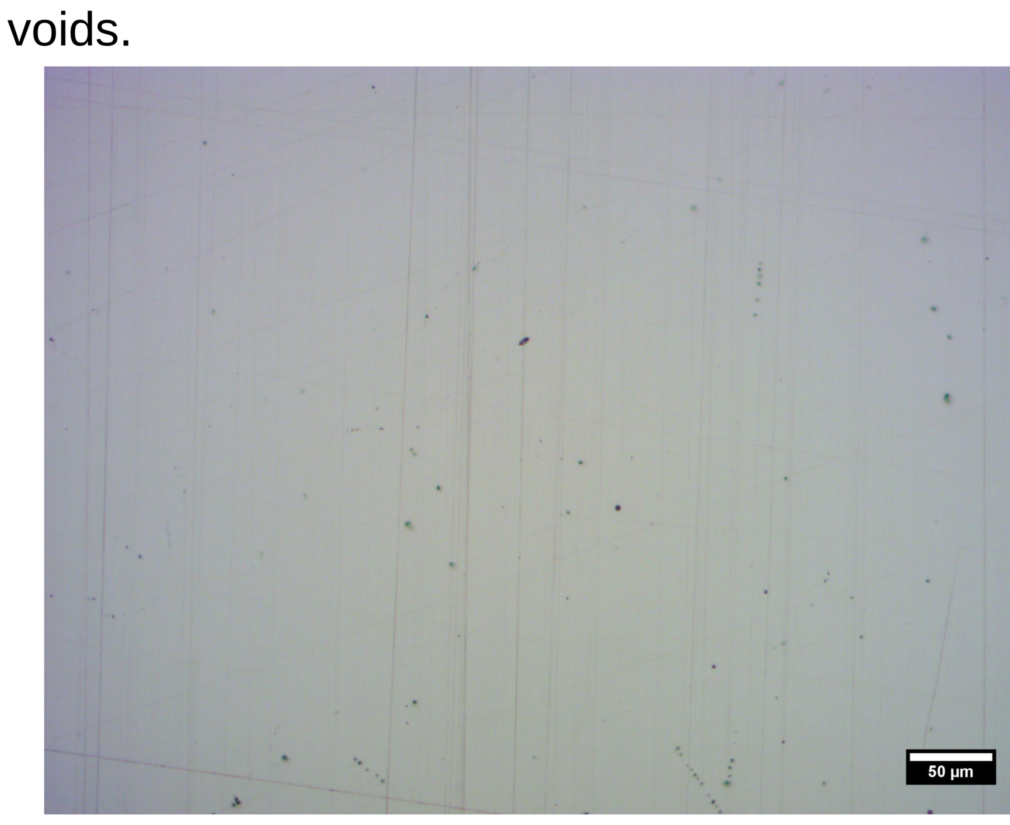

Figure 9: Optical image of a crack-free, DMLS-fabricated Alloy 230 sample from DOE 2, using 30 μm layer thickness.

Recommendations

Further research should expand on DOE 3 by manufacturing samples with parameters varying by smaller increments. Scan speed in particular should be further observed to understand the trend from lower to higher scan speeds and its effect on crack or void formation. Three new scan speeds, being 525 mm/s, 718 mm/s, and 844 mm/s, should be added to DOE 3 to get a detailed illustration of crack and void formation. Finally, to fully understand the effects of thermal stresses, temperature readings should be taken throughout the build process. To reduce thermal stresses, preheating the powder bed should be tested in order to create smaller thermal gradients during manufacturing.

References

[1] Yap, C. Y., et al. "Review of selective laser melting: Materials and applications." Applied Physics Reviews 2.4 (2015): 041101.

[2] Bauer, T., Dawson, K., Spierings, A.B., Wegener, K., (N/A). Institute for rapid product development, St. Gallen, Switzerland, and Centre for Materials and Structures, University of Liverpool, and Institute of machine tools and manufacturing, Zurich, Switzerland. *Microstructure and Mechanical Characterization of SLM processed Haynes 230.*